International Journal of Biological Macromolecules 106 (2018) 1–10

Contents lists available at ScienceDirect

International Journal of Biological Macromolecules

journal homepage: www.elsevier.com/locate/ijbiomac

Efficient removal of toxic phosphate anions from aqueous environment using pectin based quaternary amino anion exchanger

Mu. Naushad[a,*], Gaurav Sharma[b,*], Amit Kumar[b], Shweta Sharma[b], Ayman A. Ghfar[a], Amit Bhatnagar[c], Florian J. Stadler[d], Mohammad R. Khan[a]

[a] Department of Chemistry, College of Science, Building#5, King Saud University, Riyadh-11451, Saudi Arabia
[b] School of Chemistry, Shoolini University, Solan-173212, Himachal Pradesh, India
[c] Department of Environmental and Biological Sciences, University of Eastern Finland, P.O. Box 1627, FI-70211, Kuopio, Finland
[d] College of Materials Science and Engineering, Shenzhen Key Laboratory of Polymer Science and Technology, Guangdong Research Center for Interfacial Engineering of Functional Materials, Nanshan District Key Lab for Biopolymers and Safety Evaluation, Shenzhen University, Shenzhen 518060, PR China

ARTICLE INFO

Article history:
Received 25 April 2017
Received in revised form 19 July 2017
Accepted 28 July 2017
Available online 31 July 2017

Keywords:
Pectin
Exchangers
Adsorption
Phosphate anions
Spectrophotometer

ABSTRACT

Pectin based quaternary amino anion exchanger (Pc-QAE) was prepared using simple crosslinking polymerization method. This anion exchanger was characterized by X-ray diffraction (XRD), scanning electron microscopy (SEM) and Fourier transform infrared spectroscopy (FTIR). Pc-QAE was applied for the removal of phosphate anion from the aqueous solution. The adsorption process which was pH dependent showed maximum adsorption of phosphate anions at pH 7. Pc-QAE showed good monolayer adsorption capacity for phosphate anions which demonstrated its good capability towards Langmuir isotherm model. Moreover, the adsorption was evaluated thermodynamically and the negative value of Gibbs free energy (−1.791 KJ/mol) revealed the spontaneity of adsorption process. The value of ΔH° and ΔS° were found to be 15.28 and 49.48 KJ/mol, respectively representing the endothermic nature and enhancement in degree of freedom due to the adsorption process.

1. Introduction

Phosphates, which are the pertinent component of metabolism in both plants and animals, assist in the oxidation of blood in the body. They generally exist in three different forms such as orthophosphate, metaphosphate and organically bound phosphate. All these forms have different sources of origin and different applications. Wastewater from laundering agents such as soaps, detergent and shampoo contain phosphate, which is circulating as water pollutant. Approximately, laundry detergents contain 35% to 75% sodium triphosphate ($Na_5P_3O_{10}$), which serves two purposes [1–7], providing an alkaline medium (pH 9.0–10.5) for effective cleansing and to restrain calcium and magnesium ions found in water and prohibit them from interfering with the cleansing practice of the detergent. Also, phosphates can be found in a number of consumer products such as evaporated milk, water softeners, toothpastes and processed cheese, etc. They are generally non-toxic in nature but their presence in large amounts has great side effects such as eutrophication, constipation,and diarrhea, etc. Permissible limit for phosphate discharge in India is 5 mg/L as Phosphorus and in U.S. it is only 0.5–1.0 mg/L [8–10]. WHO notified that the water containing only 5 mg/L of phosphates are usage worth. Increase above the permissible limit deteriorates the water quality. Eutrophication is the maturing of a plant body under water system because of the rise in nutrient level. Addition of phosphates and nutrients to the water body by the human activities increases their aging process. This practice has created an imbalance in their growth and decay rate. In addition, it also leads to nasty odor and bad flavor of the water [11–13]. Rainfall causes different amount of phosphates to enter into the adjacent water bodies. Presence of these phosphates in permissible limits assists the growth of underwater plants which further helps in preserving the water superiority. However, if surplus amount of phosphate enters the waterway, algae and oceanic plants will grow wildly, obstruct up the waterway and consumes up ample amounts of dissolved oxygen [14–20]. Their rapid growth ultimately leads to early death and as it decays it lessens the oxygen availability. This in turn causes the downfall of aquatic life because of the lesser availability of dissolved oxygen.

Different physical, chemical and biological methods have been tested for the removal of pollutants from the waste water [21–26].

* Corresponding authors.
E-mail addresses: mnaushad@ksu.edu.sa (Mu. Naushad), gaurav8777@gmail.com (G. Sharma).

http://dx.doi.org/10.1016/j.ijbiomac.2017.07.169
0141-8130/

Expensive and low efficiency (10%) of physical methods makes them inappropriate for practical uses [27,28]. Chemical methods are also not acceptable due to their high maintenance cost and production of toxic by-products. The removal efficiency in case of biological processes is recorded to be only 30%. Researchers have suggested that adsorption can be an effective method in this case due to its inexpensive, simple and non- toxic nature [29–34].

Pectin is a naturally occurring polysaccharide present in the plant's cell walls. It functions as an intracellular and intercellular cementing material. Its biodegradable and high gelling & stabilizing nature make it a prominent material for use in many applications [31,35,36]. It has the ability of binding to a number of organic/inorganic substances with the molecular interactions.

Herein, we reported novel pectin based quaternary amino anion exchanger (Pc-QAE) for the remediation of phosphate anions from the synthetically prepared wastewater. Prepared anion exchanger was characterized by SEM, FTIR and XRD. The removal of phosphate ion was investigated using different adsorption isotherms such as Langmuir, Freundlich and Temkin. In addition, kinetic studies have also been carried out using pseudo first order and pseudo second order kinetics.

2. Materials and methods

2.1. Chemical and apparatus

Pectin (CDH), epichlorohydrin (CDH), N,N-Dimethyl formamide (LobaChemie), pyridine (CDH), triethyl amine (LobaChemie), potassium dihydrogen orthophosphate (qualigens), ammonium molybdate (Loba Chemie), sodium sulphide (CDH) and sulphuric acid (CDH). All chemicals used were of analytical grade. Electronic balance (Kerro BLC 3002), oven (NSW India), Fourier transform infrared (FTIR) spectrophotometer (Nicolet 5700 FTIR spectrophotometer), X-Ray Diffractrometer (Philips 1830 diffractometer), UV–visible spectrometer (INCO instrument and chemical private limited), scanning electron microscopy (JSM 6100), centrifuge machine (instruments, chemical private limited) were used.

2.2. Preparation of pectin based quaternary amino anion exchanger (Pc-QAE)

The anion exchanger was synthesized by adding 20 mL epichlorohydrin and 25 mL of N,N-dimethyl formamide into 6 g of pectin in a 250 mL round bottom flask. The mixture was heated at 85 °C with constant stirring for 1 h on magnetic stirrer. Batch volumes (20 mL) of catalyst i.e. pyridine was added to this mixture and solution was again heated for 1 h at 85 °C. This was followed by the addition of 25 mL of 99% triethyl amine for grafting reaction. This mixture was heated and stirred at 85 °C for 3 h. The obtained product was washed with excess of water to remove the unreacted chemicals, dried at 60 °C and was sieved.

2.3. Characterization

FTIR is a way out solution for the determination of various bonds and atoms present in organic or inorganic samples. Infrared spectrum of a molecule is produced only when the natural frequency of vibration of atoms matches the frequency of incident radiations [37,38]. After absorbing the correct wavelength of radiation, the molecule starts vibrating and gives a characteristic peak. The spectra produce a unique molecular fingerprint that can be used to scan samples. Band position in infrared may be expressed conveniently by wave number ν. Band intensities are expressed either as transmittance (T) or absorbance (A) [39–42]. FTIR spectroscopy was accomplished in the range of 400–4000 cm^{-1}. The attained data and plots were used to find the molecular structural symmetry, purity and nature of chemical bond present in synthesized material.

X-Ray diffraction is an analytical technique used primarily for the phase identification and quantitative analysis of various crystalline forms of molecules. This technique is based on the principal of constructive interference. The X-rays gets easily diffracted from materials which, are crystalline and have repeating or regular atomic structures. When X-rays interact with crystalline substance or phase, a diffraction pattern is obtained. The powder diffraction method is thus appropriate for the identification and characterization of poly-crystalline phases [43]. The easy accessibility of X-ray diffraction (XRD) makes it a useful technique not only for the phase identification, but also for the identification of lattice structure and for the modeling of basic unit.

The d spacing between diffraction planes is calculated using Bragg's diffraction

$$n\lambda = 2d\sin\theta \quad (1)$$

where, λ = wavelength of X-ray, d = inter planar spacing, θ = diffraction angle and n = 0, 1, 2, 3, etc.

Scanning electron microscope (SEM) is highly efficient tool for surface analysis that uses high energy focused electron beam that generate range of signals at the surface of solid specimens. The signals originated from electron sample interactions, reveal information about the sample including chemical composition, surface morphology and crystalline structures, etc. of the sample [44–47]. This method allows sample images to be collected in the magnification range of 10 X to 2,50,000 X. Interaction of high energy electron beam with the sample produces secondary electrons, backscattered (BSE) electrons, X-rays with characteristic energies, or photons. These emitted electrons and photons helps in analyzing the sample's surface morphology, and chemical composition. The backscattered electrons (BSE) helps in determining the composition of the sample under determination. The secondary electrons, however, are the loosely bound outer shell electrons that are ejected by inelastic collisions and helps in analyzing the surface morphology of the sample. The photons generated during the interaction can be used for the elemental detection [48–50].

2.4. Removal of phosphate anions from water by batch method

Adsorption of phosphate anions onto Pc-QAE was examined by batch adsorption method. Under this method, phosphate concentration of 50–250 mg/L was taken with 150 mg of Pc-QAE in 100 mL Erlenmeyer flasks. These flasks were sealed and agitated at 160 rpm in an incubator shaker. The pH of the solutions was maintained by the use of 0.1 M HCl/NaOH solution. The Erlenmeyer flasks were withdrawn at predetermined time intervals. The phosphate anion solutions were prepared by centrifugation operated at 3000 rpm for 8 min. Finally, the residual phosphate anion concentration was determined spectrophotometrically by ammonium molybdate colorimetric method using UV–vis spectrophotometer at an absorbance wavelength of 715 nm. In all the experiments, pectin anion exchanger dosage (20–100 mg), phosphate concentration (50–250 mg/L), pH (3–12), contact time (60–300 min) and temperature (35–55 °C) were optimized as the experimental parameters.

For the ammonium molybdate method, 1.7081 g of ammonium molybdate [$(NH_4)_6Mo_7O_{24}{\cdot}4H_2O$] was dissolved in 150 mL warm distilled water. A slightly milky solution was obtained which was allowed to cool at room temperature. It was followed by the addition of 0.25 N sulphuricacid and potassium dihydrogen orthophosphate corresponding to 0.3 ppm were added. The obtained solution was mixed with 1 mL of sodium sulphide. The solution was then kept at room temperature for 20 min. The absorbance of solution was measured at 715 nm against water.

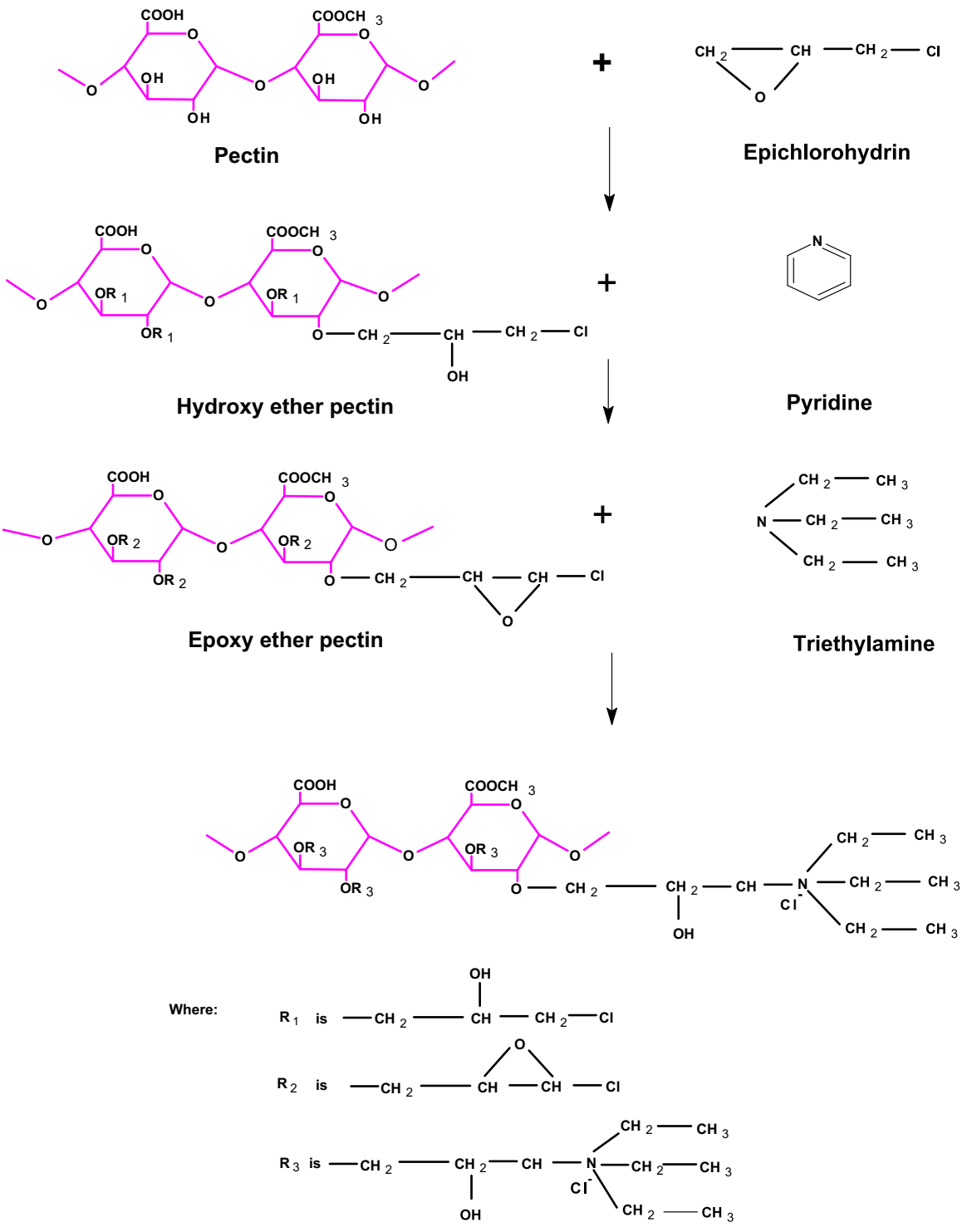

Fig. 1. Reaction mechanism for the synthesis of Pc-QAE.

3. Results and discussion

The pectin anion exchanger was synthesized by crosslinking polymerization method. Epichlorohydrin was used as a crosslinking agent and was made to react with pectin. The reaction between epichlorohydrin and pectin was carried after the hydroxyl groups in the pectin molecule got activated producing hydroxy pectin ether. The hydroxy pectin ether was then cyclized by the pyridine catalyst existing in the alkaline condition to produce the epoxy pectin ether that was used as an intermediate in the reaction. The Pc-QAE was obtained after the graft reaction between epoxy pectin ether and triethylamine. N,N-DMF was used as an organic medium which enhanced the susceptibility of the epoxide ring. Complete reaction mechanism demonstrating the synthesis of Pc-QAE and side reaction between hydroxy pectin ether & pyridine has been shown in Figs. 1 and 2, respectively.

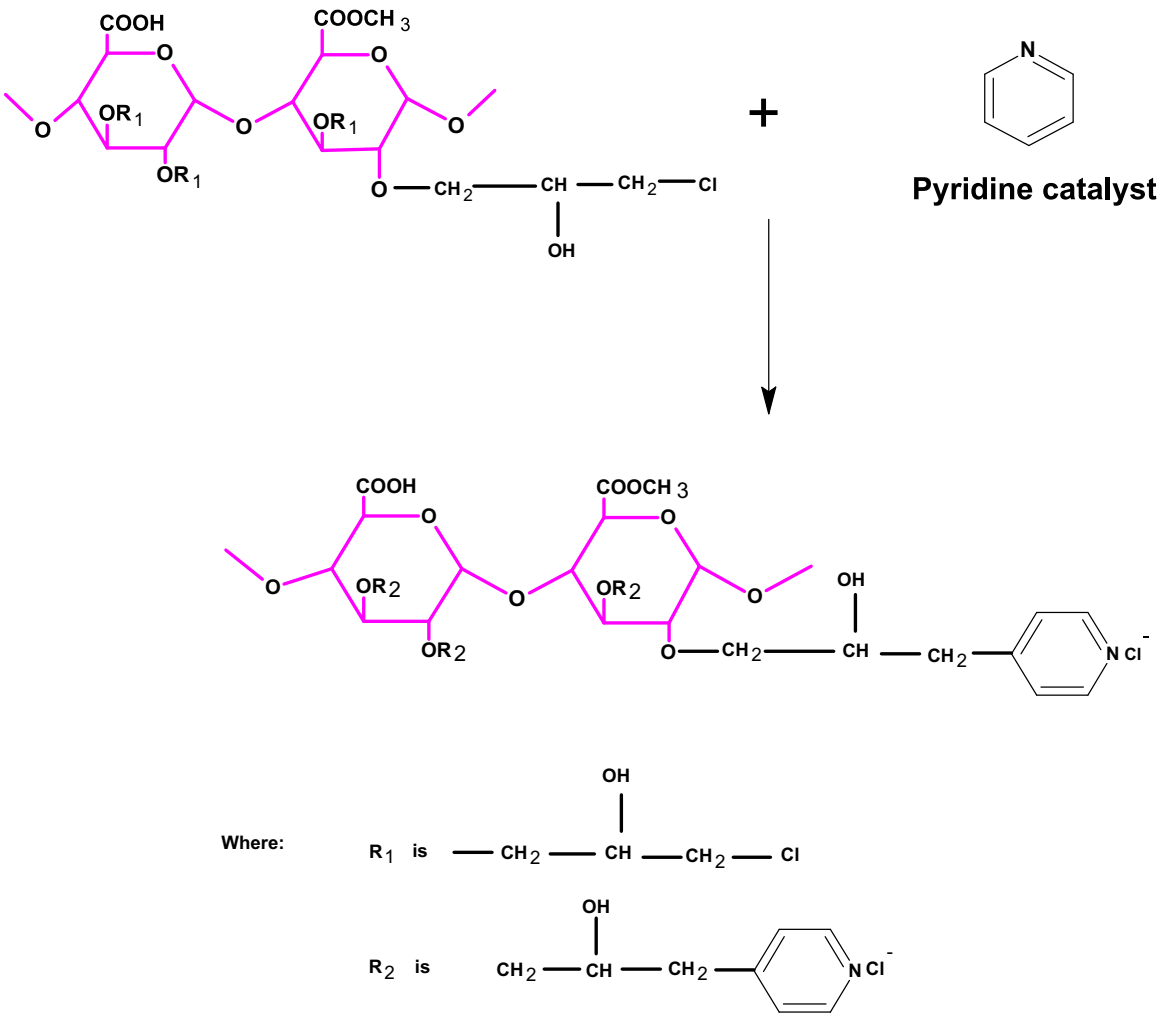

Fig. 2. Side reaction between hydroxy pectin ether and pyridine.

3.1. Characterization

FTIR technique was used to identify the functional groups present in Pc-QAE. The peaks at 1124 cm^{-1} and 3380 cm^{-1} were assigned to the C—O stretching and a mass of –OH groups. The characteristic peak of chloric alkyl in Pc-QAE by the intense vibration of band can be seen at 650 cm^{-1} [31].The intense vibration band region at 1400–1500 cm^{-1} indicated that large number of amino groups have been grafted onto the Pectin back bone [36,40]. The peak at 2974 cm^{-1} was associated with the special vibration of C—H aliphatic in pectin [42,51]. The peak at 1630 cm^{-1} showed free (—COO) carboxyl group of pectin. The change in intensity of peaks can be seen in Pc-QAE as compared to spectral peaks of pectin and triethylamine as shown in Fig. 3(a,b,c). The X-ray diffraction method has been used to determine the degree of crystallinity of anion exchanger. The non-crystalline portion simply scatters the X-ray beam to provide a continuous background, while the crystalline portion produces diffraction lines that are not continuous [33]. X-ray diffraction pattern of Pc-QAE is shown in Fig. 4. The presence of small intensity peaks showed semi-crystalline nature of Pc-QAE. Scanning electron micrographs of Pc-QAE were studied using scanning electron microscope. Fig. 5 shows the SEM images of Pc-QAE at different magnifications which indicated the rough and irregular nature of the synthesized Pc-QAE [52].

3.2. Applications of Pc-QAE for the removal of phosphate anions from aqueous medium

Adsorption of phosphate anions have been found to depend upon a number of factors such as effect of initial phosphate anion concentration, temperature, pH, contact time and adsorbent dosage. All these factors have different effect on the rate of phosphate anion adsorption.

The effect of initial anion concentration was carried out at different concentrations (50–250 mg/L) as shown in Fig. 6(a). The initial anion concentration strongly affected the adsorption of phosphate ions on the adsorbent. Adsorption is a mass transfer process that can generally be defined as accumulation of material at the interface between two phases. The amount of phosphate ions adsorbed onto Pc-QAE decreased with the increase in anion concentration [8,53,54]. The percent adsorption decreased from 55 to 20% with increase in phosphate anion concentration. This decrease in adsorption is ascribed to the decrease in the availability of adsorption sites under high phosphate anion concentration.

The effect of contact time on the amount of anion adsorbed was studied from 60 to 300 min at optimum initial concentration of phosphate solution. The extent of adsorption increased with increase in contact time due to high availability of interaction time period [45,55,56]. The adsorption efficiency attains maximum value at 300 min. The increase in adsorption in relation to the contact time is shown in Fig. 6(b).

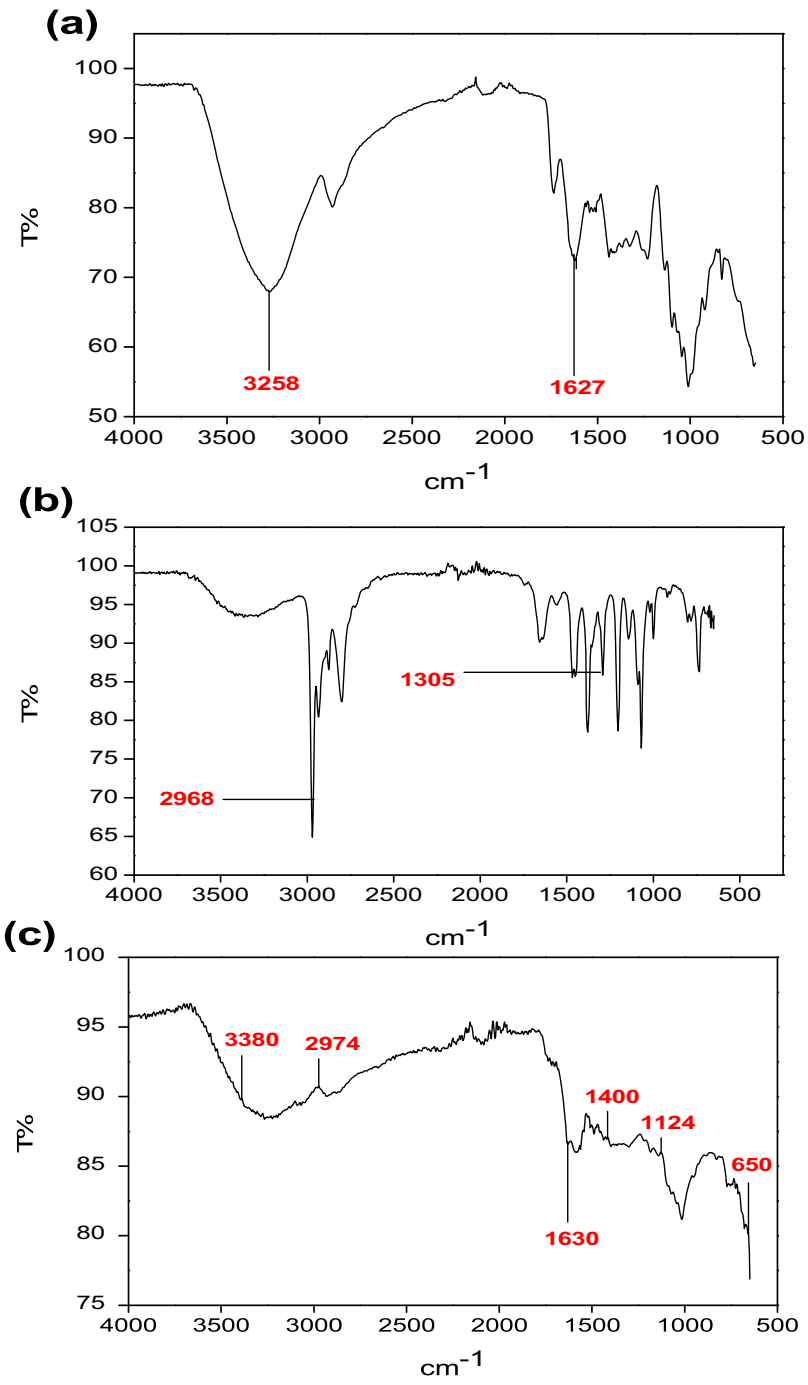

Fig. 3. FTIR images (a) pure pectin (b) triethylamine (c) Pc-QAE.

The pH of solution was a significant factor for the adsorption of phosphate anion by Pc-QAE. It is one of the key factors because it controls the electrostatic interactions between adsorbent and adsorbate. Low pH of the solution demonstrates the high concentration of H^+ ions which suppress the anionic nature of phosphate ions. As a result of which the adsorption process was quite slow [57–59]. However, at pH 7, the adsorption increased due to the presence of OH^- ions which facilitated the ion exchange process, as a result of which the adsorption process was increased. Thus, an equilibrium point was attained at pH 7 as shown in Fig. 6(c). However, with further increase in pH level, the adsorption gradually decreases and remains only 60% at pH 12.

The adsorption of phosphate anion was increased with the increase in adsorbent dosage and reached a maximum value at 100 mg of adsorbent dosage. As expected, the percentage of adsorption increased with the increase in dosage of adsorbent as shown in Fig. 6(d). This increase in adsorption was due to the accessibility of large number of vacant sites.

Temperature has important and stronger influence on the adsorption process. As the temperature increases, the rate of diffusion of adsorbate across the external boundary layer and interval pores of the adsorbent particle increases [60,61]. Generally, physical adsorption increases with fall in temperature and chemical adsorption increases with increase in temperature up to a certain value. In the present study, the effect of temperature on the adsorp-

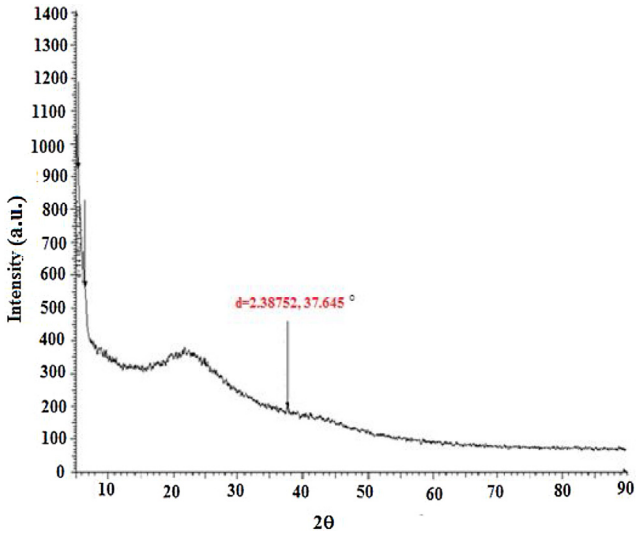

Fig. 4. XRD image of Pc-QAE.

tion was studied at 35–55 °C. Maximum uptake of phosphate (75%) was reported at 55 °C as shown in Fig. 6(e) which also confirmed that adsorption of phosphate onto Pc-QAE was chemical in nature.

3.3. Equilibrium study

The adsorption capacity of Pc-QAE was studied using various isotherm models such as Langmuir, Freundlich and Temkin. The equilibrium state helps in determining that how the adsorbate is distributed among the liquid and solid phase [62,63].

3.3.1. Langmuir isotherm

The Langmuir equation can be expressed as:

$$q_e = \frac{q_m K_L C_e}{1} + K_L C_e \quad (2)$$

where q_e ($mg\,g^{-1}$) is the amount of phosphate anion adsorbed at equilibrium, C_e ($mg\,L^{-1}$) is the concentration of phosphate in the solution at equilibrium and q_m ($mg\,g^{-1}$) and K_L ($L\,mg^{-1}$) denotes the Langmuir constants related to adsorption capacity and adsorption energy, respectively [64,65]. The constants K_L and q_m can be calculated from slope and intercept of linear plot of C_e/q_e vs. C_e as shown in Fig. 7 (a) and the calculated values are summarized in Table 1. The high correlation coefficient value (0.99) of this isotherm denoted the monolayer adsorption of phosphate anions onto Pc-QAE.

3.3.2. Freundlich isotherm

It describes the heterogeneous adsorption which is not only limited to the monolayer capacity. The linear equation for Freundlich isotherm is [66]:

$$q_e = K_f C_e^{1/n} \quad (3)$$

Where K_f and n denotes the Freundlich constants related to multilayer adsorption capacity and adsorption intensity respectively. Values of n and K_f were calculated from the slope and intercept of plot of Log q_e vs Log Ce as shown in Fig. 7(b) and the calculated values are tabulated in Table 1. According to theory, if the value of n is greater than 1, then it represents favourable adsorption. Lower correlation coefficient (R^2) value (0.85) showed the divergence of this model from the experimental data.

3.3.3. Temkin model

This model presumes that heat of adsorption decrease with the sorbate and sorbent interactions and the sorption process was char-

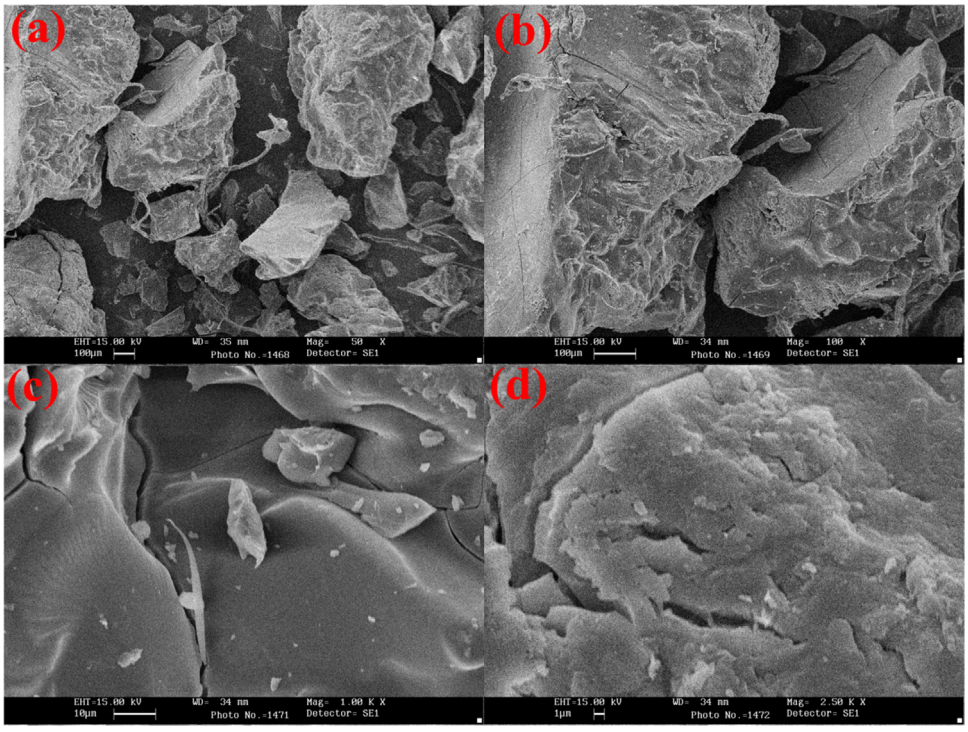

Fig. 5. SEM images of Pc-QAE at different magnifications.

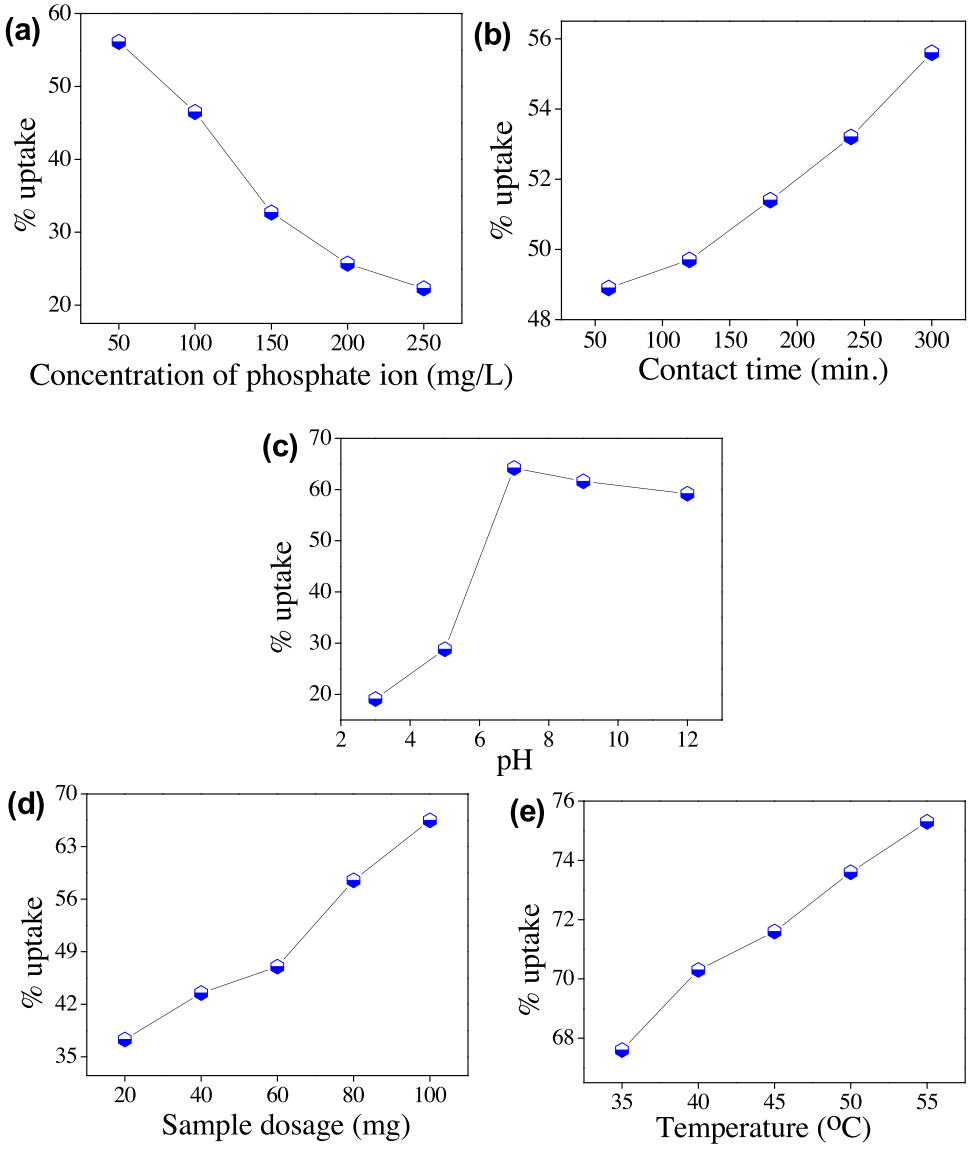

Fig. 6. Effect of (a) concentration of phosphate ion (b) contact time (c) pH (d) sample dosage and (e) temperature.

Table 1
Isotherm parameters for the adsorption of phosphate anion onto Pc-QAE.

Langmuir constants	Values	Freundlich constants	Values	Temkin constants	Values
Q_m (mg g^{-1})	31.07	K_f (mg g^{-1})	6.087	A	0.64
K_L (L mg^{-1})	0.041	n	3.35	B (mg g^{-1})	5.860
R^2	0.99	R^2	0.85	R^2	0.88

acterized by the uniform distribution of binding The linear equation for temkin model is given as:

$$q_e = B_t \ln(K_t) + B_t \ln(C_e) \quad (4)$$

where B_t denotes the heat of sorption and K_t (Lmg^{-1}) represents the equilibrium binding constant. The temkin parameters were calculated from the plot of q_e vs. lnCe as shown in Fig. 7(c) and the results are shown in Table 1. Results demonstrated lower R^2 value (0.88) as compared to Langmuir isotherm.

Out of the three adsorption isotherms, Langmuir model provide best correlation coefficient (0.99) which better discuss its suitability for adsorption of phosphate ions onto the P-QAE. Table 2 shows the comparative studies of adsorptional ability of Pc-QAE with the traditionally available different adsorbents. The results showed that Pc-QAE had better adsorption capacity in comparison to other adsorbents given in Table 2.

3.4. Adsorption kinetics

Kinetic models are of immense importance due to their ability in evaluating the time period requirement for attaining the equilibrium point in the adsorption process. It also explores the effectiveness of the adsorbent and the identification of the type of mechanisms involved in an adsorption system [64–66]. Here, pseudo first order and pseudo second order kinetics were used for evaluating the adsorption process.

Table 2
Comparison of adsorptional capacity of Pc-QAE with the traditionally available different adsorbents.

S.No.	Adsorbent	Adsorption capacity (mg/g)	Reference
1.	Fe(III)-loaded orange waste	13.94	[67]
2.	Red mud	0.58	[68]
3.	Steel slag	5.3	[69]
4.	Basic oxygen furnace (BOF) slag	4.97	[70]
5.	Pc-QAE	31.07	Present study

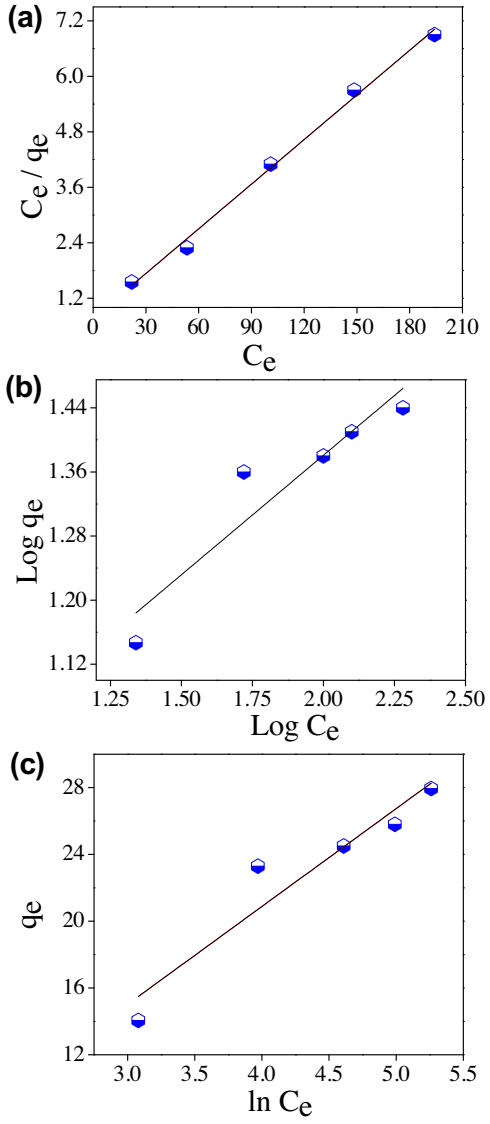

Fig. 7. (a) Langmuir (b) Freundlich (c) Temkin models for adsorption of phosphate ion onto Pc-QAE.

3.4.1. Pseudo first order kinetics

This kinetic model is based on the assumption that the adsorption rate is proportional to the no. of free sites available, occurring exclusively onto one site per ion. It is also known as Lagergren equation and is given as follows:

$$\mathrm{Log}\,(q_e - q_t) = \mathrm{Log}q_e - \left(\frac{K_1}{2.303}\right) t \quad (5)$$

Table 3
Plot parameters for adsorption kinetics and thermodynamics.

Pseudo first order	K_1 (min^{-1})	q_e ($mg\,g^{-1}$)	R^2
	0.00241	1.49	0.90
Pseudo second order	K_2 (min^{-1})	q_e ($mg\,g^{-1}$)	R^2
	0.00436	14.36	0.99
Thermodynamics	ΔG° ($kJ\,mol^{-1}$)	ΔH° ($kJ\,mol^{-1}$)	ΔS°
	−1.791	15.28	49.98

3.4.2. Pseudo second order kinetics ‘

This model is based on the theory that sorption rate is controlled by a chemical sorption mechanism involving electron transfer between adsorbate and adsorbent. This kinetic model is given as:

$$\frac{t}{q_t} = \frac{1}{k_2 q_e^2} + \frac{t}{q_e} \quad (6)$$

Here, q_t and q_e ($mg\,g^{-1}$) are the amount of phosphate anion adsorbed per unit weight of the Pc-QAE at time t and at equilibrium, respectively [48]. K_1 (min^{-1}) and k_2 ($g\,mg^{-1}\,min^{-1}$) are the pseudo first order and pseudo second order rate constants of the sorption process and t(min) is the mixing time [49,50]. The high correlation value (R^2) of the pseudo second order kinetics as compared pseudo first order kinetics as shown in Table 3indicated that the adsorption of phosphate anions was chemical in nature (Fig. 8a,b).

3.5. Adsorption thermodynamics

The thermodynamics for the adsorption of phosphate onto Pc-QAE was evaluated from free energy change (ΔG°), enthalpy change (ΔH°) and entropy change (ΔS°) of sorption using the following equations.

$$\ln K_D = -\Delta G^\circ / RT \quad (7)$$

$$K_D = C_o - C_e / C_e \quad (8)$$

$$\Delta G^\circ = -2.303 RT \log K_D \quad (9)$$

The other thermodynamic parameters such as change in standard enthalpy (ΔH°) and standard entropy (ΔS°) were determined using the following equations.

$$\Delta G^\circ = \Delta H^\circ - T\Delta S^\circ \quad (10)$$

$$\ln K_D = \Delta S^\circ / R - \Delta H^\circ / RT \quad (11)$$

where, R is a universal gas constant (8.314 (KJ/mol), C_o and C_e are the initial and equilibrium concentrations (mg/L). Different parameters determining the adsorption thermodynamics are given in Table 3.

ΔS° and ΔH° were obtained from the slope and intercept of the plot of $\ln K_D$ vs. 1/T as shown in Fig. 8(c). The positive value of ΔH° (15.28) showed the endothermic nature of adsorption process. The positive value of ΔS°(49.98 J/mol K) indicated that randomness increased at solid–liquid interface with the structural changes in the adsorbate and adsorbent molecules and also attribute to enhancement in the degree of freedom during the adsorption of phosphate ion from aqueous solution. The water molecules, which were diffused or displaced by the adsorbate molecule, gained extra

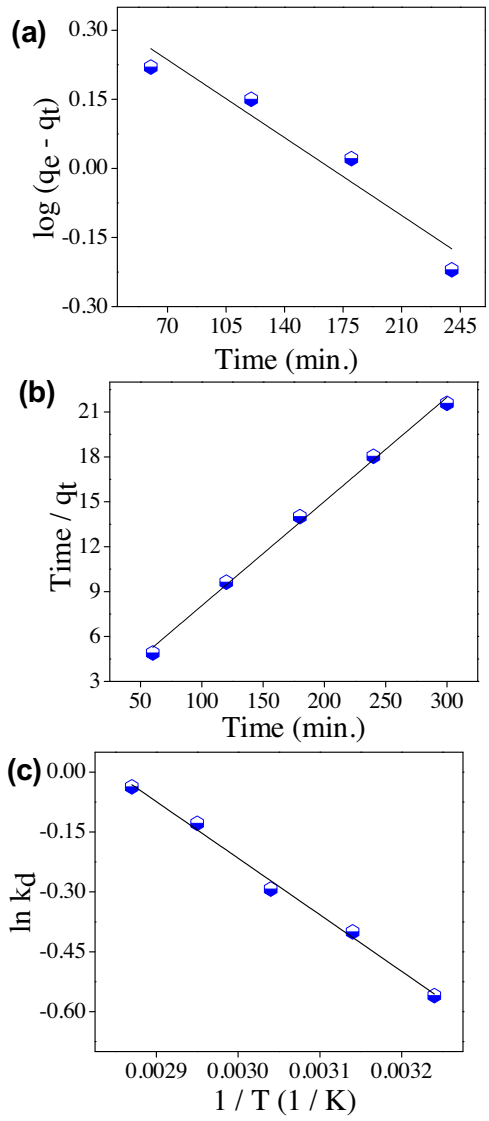

Fig. 8. (a) pseudo-first-order (b) pseudo-second–order (c) adsorption thermodynamics of phosphate ion.

amount of transitional entropy and permit the randomness in the system. The negative value of ΔG° satisfies the feasibility and spontaneity of the adsorption process.

4. Conclusion

Pectin Based quaternary amino anion exchanger (Pc-QAE) was prepared using crosslinking polymerization method and its major properties were studied. This material was used for the remediation of phosphate ions from the wastewater. The prepared anion exchanger was characterized by different techniques to explore the functional groups, bonding nature, crystal structure, size and shape. The Adsorption of phosphate anions onto Pc-QAE followed pseudo-second order kinetics and the equilibrium data fitted well with the Langmuir isotherm model indicated the monolayer adsorption. Thermodynamic results showed that phosphate anion adsorption was endothermic and spontaneous in nature.

Acknowledgement

The authors extend their appreciation to the Deanship of Scientific Research at King Saud University for funding this work through the Research Group no. RG-1436-034.

References

[1] S.H. Lee, B.C. Lee, K.W. Lee, S.H. Lee, Y.S. Choi, K.Y. Park, M. Iwamoto, Phosphorus recovery by mesoporous structure material from wastewater, Water Sci. Technol. 55 (2007) 169–176.
[2] N. Mohammadi, H. Khani, V.K. Gupta, E. Amereh, S. Agarwal, Adsorption process of methyl orange dye onto mesoporous carbon material–kinetic and thermodynamic studies, J. Colloid Interface Sci. 362 (2011) 457–462.
[3] A. Mittal, J. Mittal, A. Malviya, V.K. Gupta, Removal and recovery of Chrysoidine Y from aqueous solutions by waste materials, J. Colloid Interface Sci. 344 (2010) 497–507.
[4] E. Oguz, Removal of phosphate from aqueous solution with blast furnace slag, J. Hazard. Mater. 114 (2004) 131–137.
[5] Y. Li, C. Liu, Z. Luan, X. Peng, C. Zhu, Z. Chen, Z. Zhang, J. Fan, Z. Jia, Phosphate removal from aqueous solutions using raw and activated red mud and fly ash, J. Hazard. Mater. 137 (2006) 374–383.
[6] L. Johansson, J.P. Gustafsson, Phosphate removal using blast furnace slags and opoka-mechanisms, Water Res. 34 (2000) 259–265.
[7] F.A. Khan, A.A. Ansari, Eutrophication: an ecological vision, Bot. Rev. 71 (2005) 449–482.
[8] R. Saravanan, S. Karthikeyan, V.K. Gupta, G. Sekaran, V. Narayanan, A. Stephen, Enhanced photocatalytic activity of ZnO/CuO nanocomposite for the degradation of textile dye on visible light illumination, Mater. Sci. Eng. C 33 (2013) 91–98.
[9] A. Mittal, M. Naushad, G. Sharma, Z.A. Alothman, S.M. Wabaidur, M. Alam, Fabrication of MWCNTs/ThO_2 nanocomposite and its adsorption behavior for the removal of Pb(II) metal from aqueous medium, Desalin. Water Treat. 57 (2016).
[10] K. Fytianos, E. Voudrias, N. Raikos, Modelling of phosphorus removal from aqueous and wastewater samples using ferric iron, Environ. Pollut. 101 (1998) 123–130.
[11] R. Saravanan, V.K. Gupta, E. Mosquera, F. Gracia, Preparation and characterization of V2O5/ZnO nanocomposite system for photocatalytic application, J. Mol. Liq. 198 (2014) 409–412.
[12] K. Kadirvelu, P. Senthilkumar, K. Thamaraiselvi, V. Subburam, Activated carbon prepared from biomass as adsorbent: elimination of Ni(II) from aqueous solution, Bioresour. Technol. 81 (2002) 87–90.
[13] G. Sharma, Z.A. Alothman, A. Kumar, S. Sharma, S. Ponnusamy, M. Naushad, Fabrication and characterization of a nanocomposite hydrogel for combined photocatalytic degradation of a mixture of malachite green and fast green dye, Nanotechnol. Environ. Eng. 2 (2017) 4.
[14] S. Vasudevan, J. Lakshmi, J. Jayaraj, G. Sozhan, Remediation of phosphate-contaminated water by electrocoagulation with aluminium, aluminium alloy and mild steel anodes, J. Hazard. Mater. 164 (2009) 1480–1486.
[15] E.N. Peleka, E.A. Deliyanni, Adsorptive removal of phosphates from aqueous solutions, Desalination 245 (2009) 357–371.
[16] L. Yan, Y. Xu, H. Yu, X. Xin, Q. Wei, B. Du, Adsorption of phosphate from aqueous solution by hydroxy-aluminum, hydroxy-iron and hydroxy-iron-aluminum pillared bentonites, J. Hazard. Mater. 179 (2010) 244–250.
[17] M. Mortula, M.K. Gibbons, G. a Gagnon, Phosphorus adsorption by naturally-occurring materials and industrial by-products, J. Environ. Eng. Sci. 6 (2007) 157–164.
[18] E. Oguz, A. Gurses, M. Yalcin, Removal of phosphate from waste waters by adsorption, Water. Air. Soil Pollut. 148 (2003) 279–289.
[19] A. Afkhami, B.E. Conway, Investigation of removal of Cr(VI), Mo(VI) W(VI), V(IV), and V(V) oxy-ions from industrial waste-waters by adsorption and electrosorption at high-area carbon cloth, J. Colloid Interface Sci. 251 (2002) 248–255.
[20] V.K. Gupta, S. Agarwal, D. Pathania, N.C. Kothiyal, G. Sharma, Use of pectin–thorium (IV) tungstomolybdate nanocomposite for photocatalytic degradation of methylene blue, Carbohydr. Polym. 96 (2013) 277–283.
[21] R. Saravanan, V.K. Gupta, E. Mosquera, F. Gracia, V. Narayanan, A. Stephen, Visible light induced degradation of methyl orange using β-Ag0.333V2O5 nanorod catalysts by facile thermal decomposition method, J. Saudi Chem. Soc. 19 (2015) 521–527.
[22] R. Saravanan, M. Mansoob Khan, V.K. Gupta, E. Mosquera, F. Gracia, V. Narayanan, A. Stephen, ZnO/Ag/CdO nanocomposite for visible light-induced photocatalytic degradation of industrial textile effluents, J. Colloid Interface Sci. 452 (2015) 126–133.
[23] R. Saravanan, V.K. Gupta, V. Narayanan, A. Stephen, Visible light degradation of textile effluent using novel catalyst ZnO/γ-Mn2O3, J. Taiwan Inst. Chem. Eng. 45 (2014) 1910–1917.
[24] G. Sharma, B. Thakur, M. Naushad, A.H. Ala'a, A. Kumar, M. Sillanpaa, G.T. Mola, Fabrication and characterization of sodium dodecyl

sulphate@ironsilicophosphate nanocomposite: ion exchange properties and selectivity for binary metal ions, Mater. Chem. Phys. 193 (2017) 129–139.
[25] D. Pathania, G. Sharma, Mu. Naushad, A. Kumar, N.C. Kothiyal, Synthesis and characterization of a new nanocomposite cation exchanger polyacrylamide Ce(IV) silicophosphate: photocatalytic and antimicrobial applications, J. Ind. Eng. Chem. 20 (2014) 3596–3603.
[26] V.K. Gupta, S. Agarwal, I. Tyagi, D. Pathania, B.S. Rathore, G. Sharma, Synthesis, characterization and analytical application of cellulose acetate-tin (IV) molybdate nanocomposite ion exchanger: binary separation of heavy metal ions and antimicrobial activity, Ionics (Kiel) 21 (2015) 2069–2078.
[27] N. Mohammadi, H. Khani, V.K. Gupta, E. Amereh, S. Agarwal, Adsorption process of methyl orange dye onto mesoporous carbon material–kinetic and thermodynamic studies, J. Colloid Interface Sci. 361 (2011) 457–462.
[28] T.A. Saleh, V.K. Gupta, Processing methods, characteristics and adsorption behavior of tire derived carbons: a review, Adv. Colloid Interface Sci. 211 (2014) 93–101.
[29] V.K. Gupta, G. Sharma, D. Pathania, N.C. Kothiyal, Nanocomposite pectin Zr(IV) selenotungstophosphate for adsorptional/photocatalytic remediation of methylene blue and malachite green dyes from aqueous system, J. Ind. Eng. Chem. 21 (2015) 957–964.
[30] D. Pathania, D. Gupta, N.C. Kothiyal, G. Sharma, G.E. Eldesoky, M. Naushad, Preparation of a novel chitosan-g-poly(acrylamide)/Zn nanocomposite hydrogel and its applications for controlled drug delivery of ofloxacin, Int. J. Biol. Macromol. 84 (2016) 340–348.
[31] D. Pathania, G. Sharma, R. Thakur, Pectin @ zirconium (IV) silicophosphate nanocomposite ion exchanger: photo catalysis, heavy metal separation and antibacterial activity, Chem. Eng. J. 267 (2015) 235–244.
[32] C. Zaharia, D. Suteu, A. Muresan, R. Muresan, A. Popescu, Textile wastewater treatment by homogenous oxidation with hydrogen peroxide, Environ. Eng. Manag. J. 8 (2009) 1359–1369.
[33] R. Saravanan, V.K. Gupta, V. Narayanan, A. Stephen, Visible light degradation of textile effluent using novel catalyst ZnO/γ-Mn2O3, J. Taiwan Inst. Chem. Eng. 45 (2014) 1909–1917.
[34] D. Pathania, D. Gupta, A.H. Al-Muhtaseb, G. Sharma, A. Kumar, M. Naushad, T. Ahamad, S.M. Alshehri, Photocatalytic degradation of highly toxic dyes using chitosan-g-poly(acrylamide)/ZnS in presence of solar irradiation, J. Photochem. Photobio. A: Chem. 329 (2016) 61–68.
[35] D. Pathania, G. Sharma, M. Naushad, V. Priya, A biopolymer-based hybrid cation exchanger pectin cerium(IV) iodate: synthesis, characterization, and analytical applications, Desalin. Water Treat. 3994 (2014) 1–8.
[36] G. Sharma, M. Naushad, A.H. Al-Muhtaseb, A. Kumar, M.R. Khan, S. Kalia, M. Shweta, A. Bala, Sharma, Fabrication and characterization of chitosan-crosslinked-poly(alginic acid) nanohydrogel for adsorptive removal of Cr(VI) metal ion from aqueous medium, Int. J. Biol. Macromol. 95 (2017) 484–493.
[37] S. Karthikeyan, V.K. Gupta, R. Boopathy, A. Titus, G. Sekaran, A new approach for the degradation of high concentration of aromatic amine by heterocatalytic Fenton oxidation: kinetic and spectroscopic studies, J. Mol. Liq. 171 (2012) 153–163.
[38] L. Djoudi, M. Omari, N. Madoui, Synthesis and characterization of lanthanum monoaluminate by co-precipitation method, EDP Sci. 16 (2012) 2–9.
[39] A. Kumar, G. Sharma, M. Naushad, A. Kumar, S. Kalia, C. Guo, G.T. Mola, Facile hetero-assembly of superparamagnetic Fe_3O_4/$BiVO_4$ stacked on biochar for solar photo-degradation of methyl paraben and pesticide removal from soil, J. Photochem. Photobio. A: Chem. 337 (2017) 118–131.
[40] T.A. Saleh, V.K. Gupta, Photo-catalyzed degradation of hazardous dye methyl orange by use of a composite catalyst consisting of multi-walled carbon nanotubes and titanium dioxide, J. Colloid Interface Sci. 371 (2012) 101–106.
[41] B.S. Rathore, G. Sharma, D. Pathania, V.K. Gupta, Synthesis, characterization and antibacterial activity of cellulose acetate-tin (IV) phosphate nanocomposite, Carbohydr. Polym. 103 (2014) 221–227.
[42] D. Pathania, D. Gupta, A.H. Al-Muhtaseb, G. Sharma, A. Kumar, M. Naushad, T. Ahamad, S.M. Alshehri, Photocatalytic degradation of highly toxic dyes using chitosan-g-poly(acrylamide)/ZnS in presence of solar irradiation, J. Photochem. Photobiol. A Chem. 329 (2016) 61–68.
[43] M. Devaraj, R. Saravanan, R. Deivasigamani, V.K. Gupta, F. Gracia, S. Jayadevan, Fabrication of novel shape Cu and Cu/Cu_2O nanoparticles modified electrode for the determination of dopamine and paracetamol, J. Mol. Liq. 211 (2016) 930–941.
[44] A. Mittal, J. Mittal, A. Malviya, V.K. Gupta, Adsorptive removal of hazardous anionic dye Congo red from wastewater using waste materials and recovery by desorption, J. Colloid Interface Sci. 340 (2009) 16–26.
[45] S.A. Nabi, R. Bushra, M. Naushad, A.M. Khan, Synthesis, characterization and analytical applications of a new composite cation exchange material poly-o-toluidine stannic molybdate for the separation of toxic metal ions, Chem. Eng. J. 165 (2010) 529–536.
[46] H. Khani, M.K. Rofouei, P. Arab, V.K. Gupta, Z. Vafaei, Multi-walled carbon nanotubes-ionic liquid-carbon paste electrode as a super selectivity sensor: application to potentiometric monitoring of mercury ion(II), J. Hazard. Mater. 183 (2010) 400–409.
[47] D. Pathania, R. Katwal, G. Sharma, Fabrication, characterization and cytotoxicity of guar gum/copper oxide nanocomposite: efficient removal of organic pollutant, Mater. Sci. Forum 842 (2016) 88–102.
[48] R. Saravanan, S. Joicy, V.K. Gupta, V. Narayanan, A. Stephen, Visible light induced degradation of methylene blue using CeO_2/V_2O_5 and CeO_2/CuO catalysts, Mater. Sci. Eng. C. 33 (2013) 4725–4731.
[49] G. Sharma, A. Kumar, S. Sharma, M. Naushad, R. Prakash Dwivedi, Z.A. ALOthman, G.T. Mola, Novel development of nanoparticles to bimetallic nanoparticles and their composites: a Review, J. King Saud Univ. – Sci. (2017), http://dx.doi.org/10.1016/j.jksus.2017.06.012 (in press).
[50] G. Sharma, D. Pathania, M. Naushad, Preparation, characterization and antimicrobial activity of biopolymer based nanocomposite ion exchanger pectin zirconium(IV) selenotungstophosphate: application for removal of toxic metals, J. Ind. Eng. Chem. 20 (2014) 4482–4490.
[51] M. Naushad, T. Ahamad, G. Sharma, A.H. Al-Muhtaseb, A.B. Albadarin, M.M. Alam, Z.A.A.L. Othman, S.M. Alshehri, A.A. Ghfar, Synthesis and characterization of a new starch/SnO2 nanocomposite for efficient adsorption of toxic Hg^{2+} metal ion, Chem. Eng. J. 300 (2016) 306–316.
[52] A. Kumar, C. Guo, G. Sharma, D. Pathania, M. Naushad, S. Kalia, P. Dhiman, Magnetically recoverable ZrO_2/Fe_3O_4/chitosan nanomaterials for enhanced sunlight driven photoreduction of carcinogenic Cr(VI) and dechlorination & mineralization of 4-chlorophenol from simulated waste water, RSC Adv. 6 (2016) 13251–13263.
[53] R. Saravanan, V.K. Gupta, T. Prakash, V. Narayanan, A. Stephen, Synthesis, characterization and photocatalytic activity of novel Hg doped ZnO nanorods prepared by thermal decomposition method, J. Mol. Liq. 178 (2013) 80–93.
[54] P. Cañizares, F. Martínez, C. Jiménez, J. Lobato, M.A. Rodrigo, Comparison of the aluminum speciation in chemical and electrochemical dosing processes, Ind. Eng. Chem. Res. 45 (2006) 8749–8756.
[55] T.A. Saleh, V.K. Gupta, Synthesis and characterization of alumina nano-particles polyamide membrane with enhanced flux rejection performance, Sep. Purif. Technol. 89 (2012) 245–251.
[56] N. Adhoum, L. Monser, N. Bellakhal, J.-E. Belgaied, Treatment of electroplating wastewater containing Cu^{2+}, Zn^{2+} and Cr(VI) by electrocoagulation, J. Hazard. Mater. 112 (2004) 207–213.
[57] Z.H. Lu, E. Donner, R.Y. Yada, Q. Liu, Physicochemical properties and in vitro starch digestibility of potato starch/protein blends, Carbohydr. Polym. 154 (2016) 214–222.
[58] R. Saravanan, F. Gracia, M.M. Khan, V. Poornima, V.K. Gupta, V. Narayanan, A. Stephen, ZnO/CdO nanocomposites for textile effluent degradation and electrochemical detection, J. Mol. Liq. 209 (2015) 374–380.
[59] N. Barka, S. Qourzal, A. Assabbane, A. Nounah, Y. Ait-Ichou, Removal of Reactive Yellow 84 from aqueous solutions by adsorption onto hydroxyapatite, J. Saudi Chem. Soc. 15 (2011) 263–267.
[60] V.K. Gupta, T.A. Saleh, Sorption of pollutants by porous carbon, carbon nanotubes and fullerene- An overview, Environ. Sci. Pollut. Res. 20 (2013) 2821–2843.
[61] G. Sharma, M. Naushad, A. Kumar, S. Rana, S. Sharma, A. Bhatnagar, F.J. Stadler, A.A. Ghfar, M.R. Khan, Efficient removal of coomassie brilliant blue R-250 dye using starch/poly (alginic acid-cl-acrylamide) nanohydrogel, Process Saf. Environ. Prot. 109 (2017) 301–310.
[62] V.K. Gupta, R. Kumar, A. Nayak, T.A. Saleh, M.A. Barakat, Adsorptive removal of dyes from aqueous solution onto carbon nanotubes: a review, Adv. Colloid Interface Sci. 193–194 (193) (2013) 24––.
[63] T.M. Maryam Ahmadzadeh Tofighy, Adsorption of divalent heavy metal ions from water using carbon nanotube sheets, J. Hazard. Mater. 185 (2011) 140–147.
[64] M. Naushad, S. Vasudevan, G. Sharma, A. Kumar, Z.A. ALOthman, Adsorption kinetics isotherms, and thermodynamic studies for Hg^{2+} adsorption from aqueous medium using alizarin red-S-loaded amberlite IRA-400 resin, Desalin. Water Treat. 57 (2016) 18551–18559.
[65] M. Naushad, Z.A. ALOthman, G. Sharma, Inamuddin, Kinetics, isotherm and thermodynamic investigations for the adsorption of Co(II) ion onto crystal violet modified amberlite IR-120 resin, Ionics 21 (2015) 1453–1459.
[66] J. Febrianto, A.N. Kosasih, J. Sunarso, Y.-H. Ju, N. Indraswati, S. Ismadji, Equilibrium and kinetic studies in adsorption of heavy metals using biosorbent: a summary of recent studies, J. Hazard. Mater. 162 (2009) 616–645.
[67] B.K. Biswas, K. Inoue, K.N. Ghimire, S. Ohta, H. Harada, K. Ohto, H. Kawakita, The adsorption of phosphate from an aquatic environment using metal-loaded orange waste, J. Colloid Interface Sci. 312 (2007) 214–223.
[68] W. Huang, S. Wang, Z. Zhu, L. Li, X. Yao, V. Rudolph, F. Haghseresht, Phosphate removal from wastewater using red mud, J. Hazard. Mater. 158 (2008) 35–42.
[69] J. Xiong, Z. He, Q. Mahmood, D. Liu, X. Yang, E. Islam, Phosphate removal from solution using steel slag through magnetic separation, J. Hazard. Mater. 152 (2008) 211–215.
[70] Y. Xuea, H. Hou, S. Zhu, Characteristics and mechanisms of phosphate adsorption onto basic oxygen furnace slag, J. Hazard. Mater. 162 (2009) 973–980.